VI International Conference on Computational Methods in Marine Engineering
MARINE 2015
F. Salvatore, R. Broglia and R. Muscari (Eds)

PARAMETRIC-ADJOINT APPROACH FOR THE EFFICIENT OPTIMIZATION OF FLOW-EXPOSED GEOMETRIES

MATTIA BRENNER[*], STEFAN HARRIES[*], JÖRN KRÖGER[†] AND THOMAS RUNG[†]

[*] FRIENDSHIP SYSTEMS AG
Benzstr. 2, 14482 Potsdam, Germany
e-mail: brenner@friendship-systems.com, www.caeses.com

[†] Inst. Fluid Dynamics and Ship Theory (M8)
Hamburg University of Technology (TUHH)
Am Schwarzenberg-Campus 4, 21073 Hamburg, Germany
e-mail: joern.kroeger@tuhh.de, www.tuhh.de

Key words: Hull Form Optimization, Adjoint RANS CFD, Parametric Modelling

Abstract. Today, the optimization of ship hulls and appendages, including energy-saving devices, is typically undertaken by means of coupling parametric modelling (variable geometry) and Computational Fluid Dynamics (CFD). A relatively new approach is based on parameter-free solutions, solving the adjoint RANS equations for selected objective functions (like drag and lift). Combining parametric and parameter-free solutions is an emerging technique that helps to effectively optimize shapes without leaving the CAD domain of the model, making it easier to integrate in the overall design process.

On the basis of the Computer Aided Engineering (CAE) software CAESES, a parametric-adjoint approach will be presented. The approach is built on concatenating so-called "design velocities" and "adjoint shape sensitivities". Design velocities yield regions of influence from a pure geometric point of view within a given parametric model. Meanwhile, adjoint shape sensitivities show where and how changes of the surface affect the objective. Overlaying the surface distributions of both the design velocities and the adjoint shape sensitivities result in so-called "parametric sensitivities." These help to understand the importance of all parameters within the chosen model.

This approach will be demonstrated on a practical hull form optimization example.

1 INTRODUCTION

Using parametric modelling in the design process allows for an efficient variation of the geometry, see [1], [2]. The total number of shape-defining parameters for a typical parametric model of a flow-exposed geometry like a ship hull in the CAE platform CAESES is usually within the range of 20 to 50. This means that for complex free-form geometries the number of degrees of freedom is still so large that when using a direct optimization approach, taking into account all parameters, a high number of function evaluations, i.e. CFD computations, would be necessary to identify trends with respect to the necessary geometry modifications leading

to an improvement of the considered objective function(s). Because of the long computation times, this approach becomes infeasible, especially when dealing with complex flow situations.

In order to adapt the expenses to the available resources, the design engineer would typically select a suitable subset of parameters, either based on his experience or his technical intuition. Besides the disadvantage of reducing the available design space for the optimization, the selection of this parameter subset is often difficult, since the effect on the objective function is not known a priori. This is especially true when the engineer does not have enough experience to make a meaningful selection or when the model was produced by someone else, introducing the additional uncertainty of the specific impact of every parameter on the geometry.

The goal of the developments outlined in this paper was to implement a method that would allow optimising complex parameterized freeform geometries under consideration of the complete design space, i.e. all model parameters, with a relatively low computational expense.

2 ADJOINT CFD

The decisive information for the flow optimization of a given geometry is the correlation between the objective function J and the form parameters α_i. This correlation can be mathematically expressed through the so-called sensitivities – the rate of change (i.e. the gradient) of the objective when varying the form parameters. The individual sensitivities can be approximated by the finite difference quotient, which for n parameters in a classical gradient based optimization approach would require $n+1$ CFD computations to evaluate the corresponding modified geometry for every form parameter. As mentioned above, this direct approach is therefore not really applicable for a high number of parameters and expensive simulations. Of course, intelligent DoE strategies can possibly reduce the number of function evaluations, but they still significantly scale with the number of free parameters.

So-called adjoint methods, however, go the reverse way. Instead of evaluating the change in objective function due to a variation of parameter value, the required variation of the parameter values for a desired change in objective function is computed. Within a single computation, the adjoint method will yield the full gradient of the objective function, irrespectively of the number of parameters. The full analysis would require a conventional (primal) CFD computation, followed by one adjoint computation for each considered objective (see Figure 1).

In the context of shape optimization, the adjoint analysis will provide the so-called shape sensitivity as a result. This is given as field information on the surface of the model and describes the change of objective function due to normal displacement of the surface cells ($\partial J/\partial n_k$). A positive value of the shape sensitivity indicates a local displacement in positive normal direction and vice-versa.

The sensitivity is given by the adjoint analysis with respect to the CFD discretisation of the model surface. For industry-relevant cases, the CFD geometry is typically described by ten thousands of nodes, and therefore degrees of freedom, so that the obtained sensitivity is described with a very high degree of detail, in a quasi-continuous way. In a CAD-free approach, this information can be directly used for a displacement of the grid nodes and, therefore, a deformation of the initial geometry. When using this approach, however, a

disadvantage is given by the fact that the shape modifications are difficult to feed back into the design process and geometrical constraints (e.g. due to production restrictions) can be violated. This leads to the motivation of developing a method that maps these initial sensitivities for the degrees of freedom of the CFD geometry to the corresponding sensitivities $\partial J/\partial \alpha_i$ (rate of change of the objective function due to change of parameter values) of the CAD model parameters.

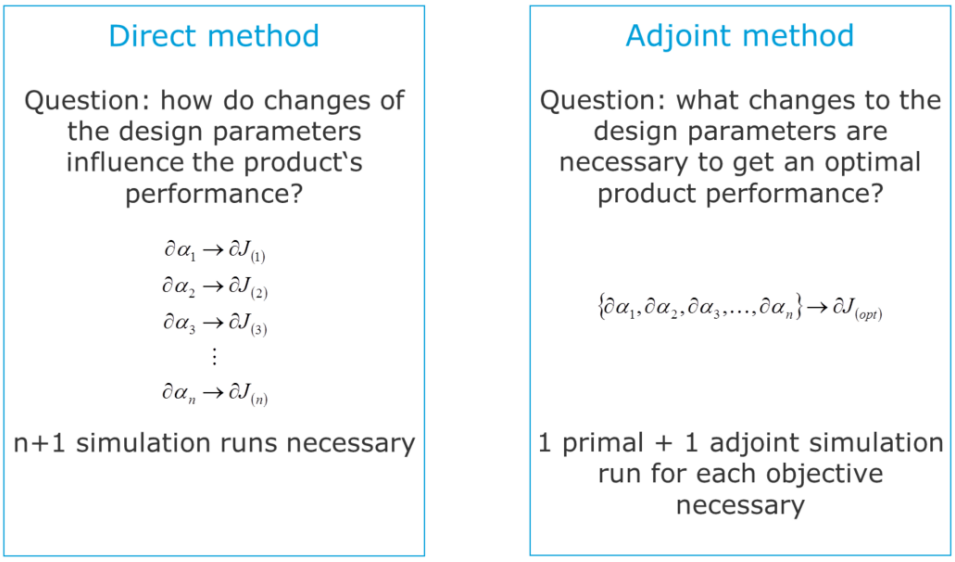

Figure 1: Comparison of direct and adjoint method

3 MAPPING ADJOINT SHAPE SENSITIVITIES TO CAD MODEL PARAMETERS

In order to map the adjoint shape sensitivities to the CAD model parameters, a new object – the *Sensitivity Computation* – that takes care of all the necessary steps, was implemented into the design platform CAESES. Initially, the adjoint sensitivities are interpolated from the CFD discretisation to the surface tessellation of the CAD model. Then, the local normal displacement of the model surface due to parameter variation – $\partial n_k/\partial \alpha_i$, the so-called design velocity – has to be determined. By tracking the dependencies for all model surfaces selected for this operation, all influencing parameters are automatically determined. These are perturbed by an individually adjustable amount in positive and negative direction and the normal displacements of the surface tessellation nodes are evaluated. For each element, the gradient $\partial n_k/\partial \alpha_i$ can then be computed from the displacement due to the perturbation. Like the adjoint shape sensitivity $\partial J/\partial n_k$, this data can be visualized as a plot on the model surface.

By comparing the two plots, one can already get a more or less good visual estimation about which parameters influence areas with high shape sensitivity and, therefore, have a more pronounced impact of the objective function. A more precise statement can be obtained by creating the product of $\partial J/\partial n_k$ and $\partial n_k/\partial \alpha_i$ for every tessellation element, weighting it with the local area, creating the sum over the surface and thereby computing the sensitivity $\partial J/\partial \alpha_i$ for every parameter (see Figure 2). These scalar values for all involved parameters are collected and displayed in a table. They show the user which of the parameters have the biggest influence on the objective function and in which direction they should be changed in

order to have a positive influence on the objective. This gradient information can be used to select a subset of the most influential parameters, as well as for a subsequent automated optimization process. In the former case, the parameter values can be manually changed or involved in a conventional optimization. In the latter case, the parameter sensitivity vector can be multiplied by a step size factor and added to the initial parameter values, thus reducing the optimization problem to a one-dimensional search. A suitable algorithm can then be used to determine the appropriate step size.

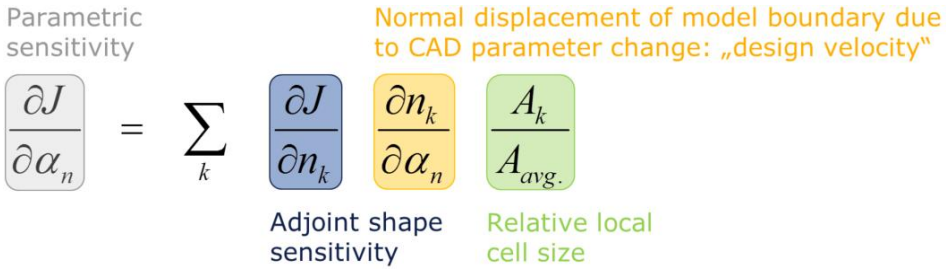

Figure 2: Calculation of parametric sensitivities

4 TEST CASE

The study presented in this paper refers to a single-screw bulk carrier. The main dimensions of the vessel are: length app. 180m (LPP 172m); beam 30m; draught 9.5m.

The vessel is simulated in self-propelled condition at a model-scale Reynolds number of $Re = 1.8 \cdot 10^8$, employing an iterative bodyforce model to adapt the propeller thrust to the total resistance that includes the propeller-hull interaction. Further details on the bodyforce propeller model are given in [3]. The bodyforces are distributed in a sub-volume Ω_P, centred 3.35m in front of the A.P., the shaft line lies 3.3m above the base line. The thickness of the propeller disk is 0.7m, the outer and inner radii are 6.2m and 1.4m, respectively. The sub-volume Ω_{obj} to evaluate the wake objective function is located 4.15m in front of A.P. with a thickness of 0.5m and outer / inner radii of 6.2m and 2.8m. The discrete objective function is evaluated on 10 concentric rings.

The free surface is replaced by a symmetry plane. The hull is symmetric with regards to the midship plane, thus only half of the vessels geometry is modelled. The computational mesh consists of 1.6M hexahedral cells and is locally refined around the aftship and in the propeller region where the primal and adjoint body forces are applied and the wake objective function is evaluated. The average near-wall spacing is 0.1m in tangential and $1.5 \cdot 10^{-2}$m in normal direction. The surface of the vessel is resolved by 70.000 cell faces. The k-Ω-MSST turbulence model is applied in conjunction with high-Re wall boundary conditions.

4.1 Parametric Geometry Model

The hull is described by a set of parameters, some of which have a global influence (length, depth etc.), whereas others cause local changes of the geometry, such as the local frame character.

The geometry model of the vessel's hull is based on CAESES' proprietary *Meta Surface* technology, which allows for a flexible generation and parameterization of complex freeform

surfaces. For the different areas of the hull, characteristic sections of the surface, mostly frames (constant x), are topologically described in so-called feature definitions [2]. In this context, features are high-level geometrical entities that encapsulate several work steps and can therefore describe a topology composed of several primitive geometry entities. A feature definition is essentially composed of list of input parameters, a script-like process description that specifies how the input is used and an output that contains the objects created within the script. The input parameters are accessible to the user in the GUI and instances of the feature can be created by entering value combinations. Input parameters for the generation of a surface section can be of positional, differential (angles) and integral (areas and centroids) nature. A typical example for an integral section parameter well-known to naval architects is the sectional area. When the values for the input parameters are given as continuous distributions in form of parametric curves (see Figure 3) – like the sectional area curve for the given example – the exact shape of the section is known at any arbitrary position within the range of the curves and a surface – the *Meta Surface* – can be generated (see Figure 4). As a consequence of this special surface description method that combines information in two particular directions, the freeform surface is fully described and controllable by parameters.

An STL-based discretised surface model of the computational domain is exported to the HEXPRESS grid generator. Following the primal/adjoint solution process, the CAD model is updated and the new computational domain is meshed with a similar mesh quality.

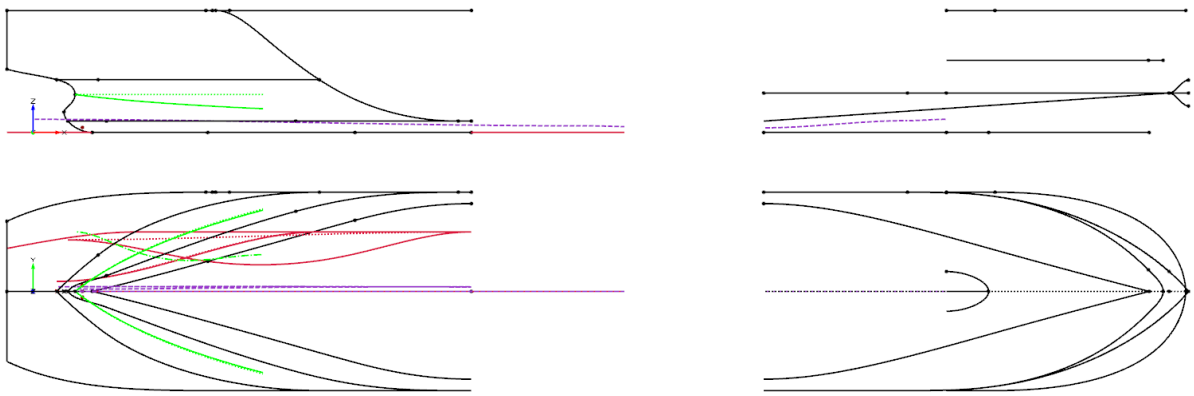

Figure 3: Longitudinal curves for the bulk carrier hull

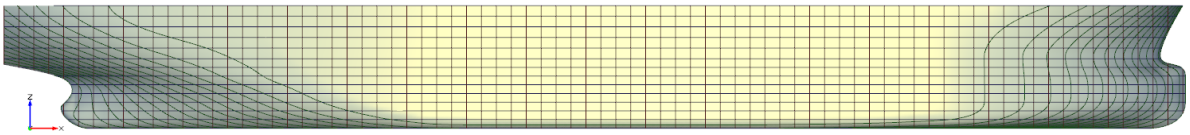

Figure 4: Surface of the bulk carrier hull

4.2 Computational Model

The numerical simulations of the present study were performed with the finite-volume Navier-Stokes solver FreSCo$^+$ [4]. The segregated algorithm is based on the strong conservation form of the momentum equations and employs a cell-centred, collocated storage

arrangement for all transport properties. Structured and unstructured meshes of arbitrarily shaped polyhedral cells are supported. The parallel numerical framework features modules for dynamic goal-oriented grid-adaptation, overset grids and deforming meshes. The implicit numerical approximation is second-order accurate in space and time. Pressure-velocity coupling is realized by the SIMPLE pressure correction scheme. Turbulence modelling is provided by various statistical (RANS) or scale-resolving (DES, LES) turbulence-models. A VOF-type mixture-fraction approach allows to model multi-phase flows. Cavitation induced mass transfer between liquid and vapour is provided by a number of Eulerian and Langrangian models. The implemented domain decomposition approach ensures parallel efficiency down to about 15.000 cells per core.

The primal RANS solver is extended by its parallelised adjoint complement [5]. The implementation of the adjoint solver reuses the primal modules and operators that are optionally reformulated to reflect the specific requirements of the adjoint formulation. This leads to an efficient, modular composition of the adjoint solver. The chosen modular approach avoids introducing redundant code and significantly simplifies code-maintenance. The consistency of the primal and the adjoint discretisation (duality) is assured on the level of the individual building blocks of the procedure. The considered adjoint framework is confined to the momentum and pressure equations and thus follows the well-known "frozen-turbulence" approach. The primal turbulence field is recalculated after each design update.

This paper focuses on the coupling of the CAE framework CAESES to the Navier-Stokes solver FreSCo$^+$. As alternative to the CAD-based optimisation approach, FreSCo$^+$ features an integrated CAD-free optimisation procedure. The CAD-free optimisation procedure comprises modules for the smoothing of the raw sensitivities, the calculation of a symmetry conform boundary deformation field, the superposition of geometric constraints and a PDE-based method to calculate the volume mesh displacement. An automated optimisation process adapts the shape of the design object in a sequence of successive executions of the primal and the adjoint RANS solver. This approach allows exploiting the full dimensionality of the design space but results in optimised geometries that have to be transferred back into the design process and that might not be feasible from a technical perspective.

Similar to the CAD-free optimisation procedure, the CAD-based optimisation cycles between the primal and the adjoint RANS solver. The geometry update is realised in the CAE framework after mapping the cell-based sensitivities to the CAD-parameters. Following the export of the new computational domain a new computational mesh is created to facilitate the evaluation of the updated design during the next optimisation step.

4.3 Objective Function

The optimisation applied to this case study was aimed at improving the operating conditions of the propeller. Here, the focus lies on the uniformity of the axial inflow to the propeller disk. The motivation is to reduce variations in the blade angle of attack that are associated with varying axial inflow conditions and can lead to noise and vibrations and may provoke cavitation.

An objective volume Ω_{obj} is declared directly in front of the propeller disk; in this subdomain a volume based objective function is integrated to evaluate the inflow quality. The results presented here refer to a wake objective function formulated by the Potsdam ship

model basin (SVA). It evaluates the deviation $\mathcal{D}_I(r)$ of the axial inflow velocity u^a from its radial mean value $\bar{u}^a(r)$

$$\mathcal{D}_I(r) = \frac{1}{2\pi u_S} \int_0^{2\pi} |u^a(r) - \bar{u}^a(r)| d\Theta \quad \text{for } r_i < r < r_o \,, \tag{1}$$

$$\text{with} \quad \bar{u}^a(r) = \frac{1}{2\pi} \int_0^{2\pi} u^a(r)\, d\Theta \quad \text{for} \quad r_i < r < r_o \,. \tag{2}$$

Besides, the relative velocity bandwidth $\mathcal{D}_{II}(r)$ that is experienced on a certain propeller radius is incorporated in the wake objective function

$$\mathcal{D}_{II}(r) = \frac{1}{u_S} (\max(u^a) - \min(u^a)) \,. \tag{3}$$

The optimisation aims to maximize the wake objective function

$$J = 1 - \frac{1}{r_o - r_i} \int_{r_i}^{r_o} \sqrt{2\ \mathcal{D}_I(r)\ \mathcal{D}_{II}(r)}\ \mathrm{dr} \,. \tag{4}$$

A more detailed discussion of the components of the wake objective function and its evaluation on unstructured computational meshes is given in [6].

4.4 Adjoint RANS

The flow is modelled by the Reynolds-averaged incompressible Navier-Stokes equations

$$\rho u_j \frac{\partial u_i}{\partial x_j} = \frac{\partial}{\partial x_j} \left(2\mu_{eff} S_{ij} - p\delta_{ij}\right) + f_i \quad \text{and} \quad \frac{\partial u_j}{\partial x_j} = 0 \quad \text{in} \quad \Omega \,. \tag{5}$$

Here ρ, μ_{eff}, u_i, S_{ij}, p and f_i are the fluid density and effective dynamic viscosity, the velocity components, the strain-rate tensor, the pressure and the body-force components. As discussed in [5] and [7], the corresponding adjoint PDE read

$$-\rho u_j \frac{\partial \hat{u}_i}{\partial x_j} = \frac{\partial}{\partial x_j} \left(2\mu_{eff} \hat{S}_{ij} - \hat{p}\delta_{ij}\right) - \rho \hat{u}_j \frac{\partial u_j}{\partial x_i} - \frac{\partial j}{\partial u_i} \quad \text{and} \quad \frac{\partial \hat{u}_i}{\partial x_i} = 0 \,. \tag{6}$$

The adjoint equations are solved for the adjoint variables ($\hat{u}_i$, $\hat{p}$) and are specific to the objective function. The advective coupling of the adjoint momentum equations is realised by considering a face-based formulation that is derived from the discretisation of the primal convective momentum flux. The volume-based objective function considered for the present

study is introduced via adjoint source terms in the adjoint momentum equation. Following a reformulation to facilitate an evaluation on unstructured meshes [6], the chosen SVA wake objective function leads to

$$\delta J = \int_{\Omega_{obj}} \delta u_i \frac{\partial j}{\partial u_i} d\Omega \qquad \text{with} \tag{7}$$

$$\frac{\partial j}{\partial u_i} = -\tilde{e}_i^a \frac{C}{2} \frac{u^a - \bar{u}^a(r)}{r} \sqrt{\frac{u_S \, \mathcal{D}_{II}(r)}{\max(|u^a - \bar{u}^a(r)|^3, \epsilon)}} \quad , \qquad C = \left[u_S \int_{\Omega_{obj}} \frac{d\Omega}{r} \right]^{-1} . \tag{8}$$

4.5 Results

As a first step, primal and adjoint solution were computed for the baseline geometry of the hull. The objective function for this initial design resulted in a value of 0.75103. The adjoint sensitivity field on the hull surface can be seen in Figures 5 and 6, where it is compared to the design velocities for two of the parameters that were selected for the optimization. In total, 12 parameters were used in this optimization, which encompasses all parameters that have an influence on the skeg shape. Due to their very different magnitude and range size, the parameters were normalized to the range between upper and lower bound (which were set to reasonable values) and subjected to the sensitivity analysis as outlined in Section 3. An exemplary parameter sensitivity table for one of the optimization steps is shown in Figure 7.

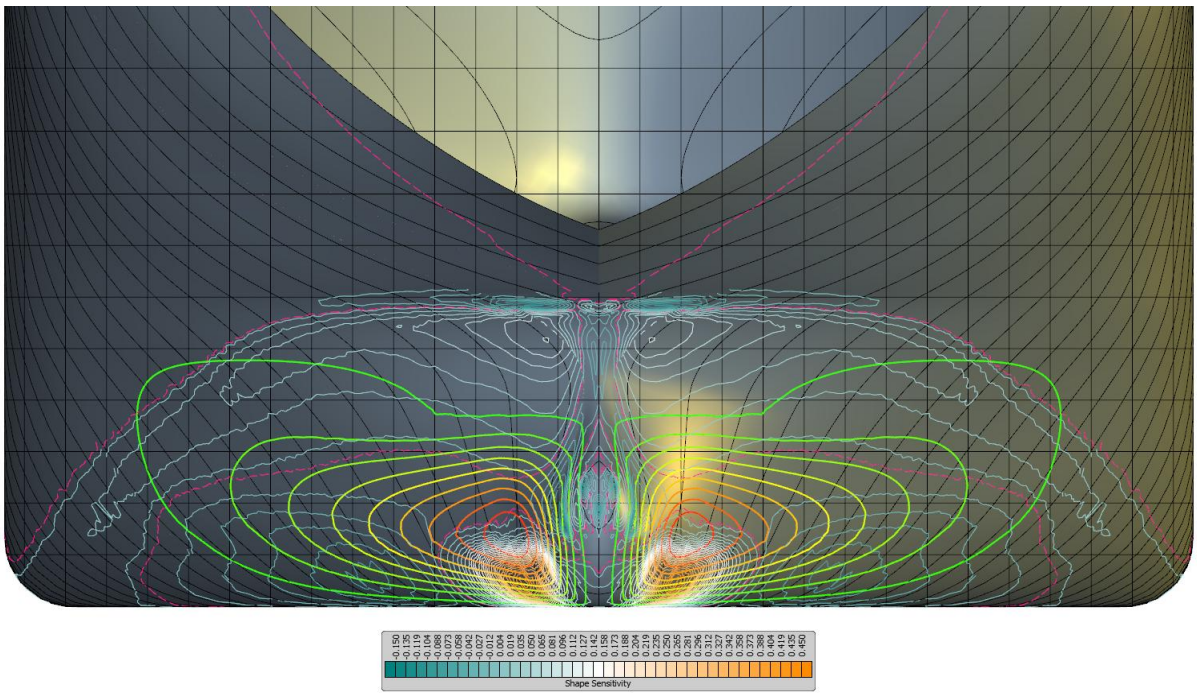

Figure 5: View of the ship's aftbody with plotted adjoint shape sensitivity (teal to orange colour map, dashed pink line represents shape sensitivity equal to 0) and design velocity (blue to red colour map, range of green to red indicating positive values) for a parameter with a high parametric sensitivity

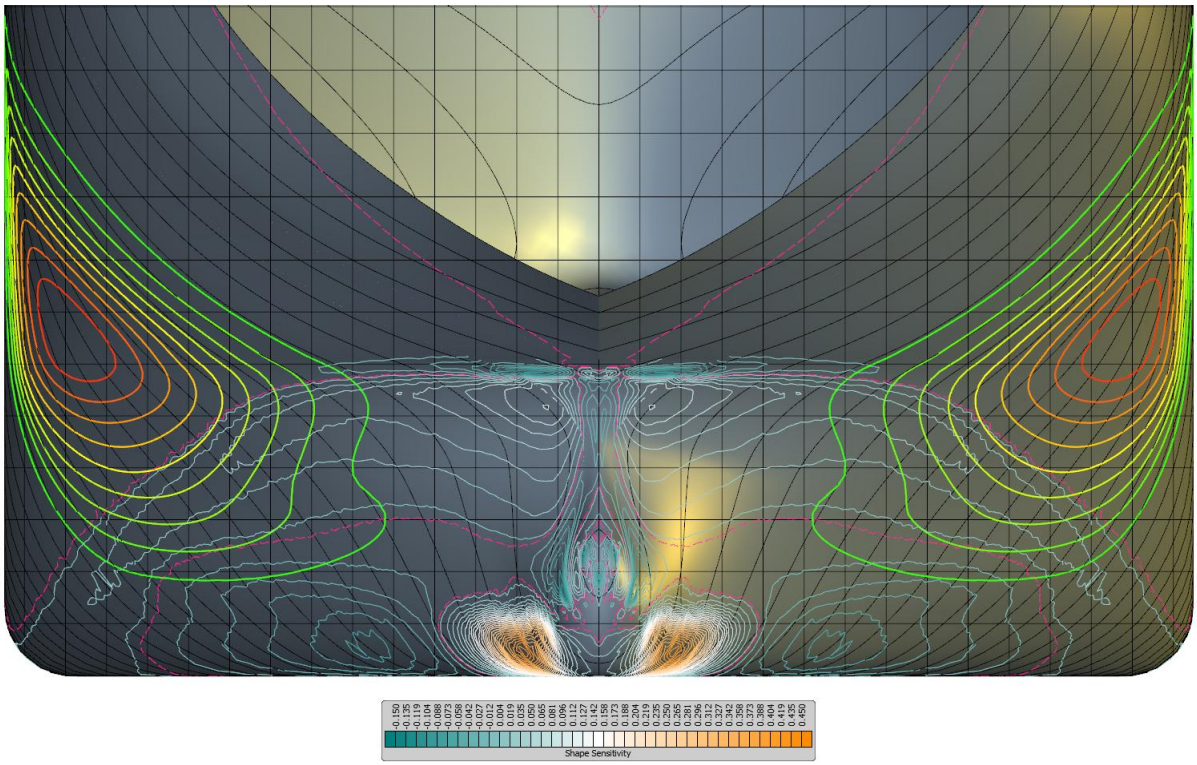

Figure 6: View of the ship's aftbody with plotted adjoint shape sensitivity (teal to orange colour map, dashed pink line represents shape sensitivity equal to 0) and design velocity (blue to red colour map, range of green to red indicating positive values) for a parameter with a low parametric sensitivity

vers2_mod1: Sensitivities

	Sensitivity	Variation Delta
CPCFullnessPart4_norm	0.779167	0.0001
WL2FullnessFwd_norm	0.77508	0.0001
diagAngle_norm	0.261984	0.0001
diagFullness_norm	3.38109	0.0001
diagTanAft_norm	1.5776	0.0001
xAftBase_norm	-16.7834	0.0001
xRelWL2Int_norm	-0.370241	0.0001
xWL1IntAft_norm	-20.7753	0.0001
xWl1IntFwd_norm	-1.36425	0.0001
yRelWL2Int_norm	0.496294	0.0001
yWL1IntAft_norm	12.3389	0.0001
yWL1IntFwd_norm	2.22798	0.0001

Figure 7: Parameter sensitivities

To obtain the next geometry variant, the parameter sensitivity value for each parameter was multiplied with a common step size and added to the current parameter value. The step size was set so that the maximum displacement of the hull surface was approximately 10cm.

This procedure was iteratively repeated five times and resulted in a stepwise improvement of the objective function up to a value of 0.75286 (see Figure 10). Because only the skeg parameters were considered in this case study and the total geometry changes were rather large in the end, the hull part above the skeg was manually adapted (adjustment of 2 parameter values) to better fit the significantly narrower skeg (see Figure 8). This resulted in a further, surprisingly large, improvement of the objective function to a value of 0.76073.

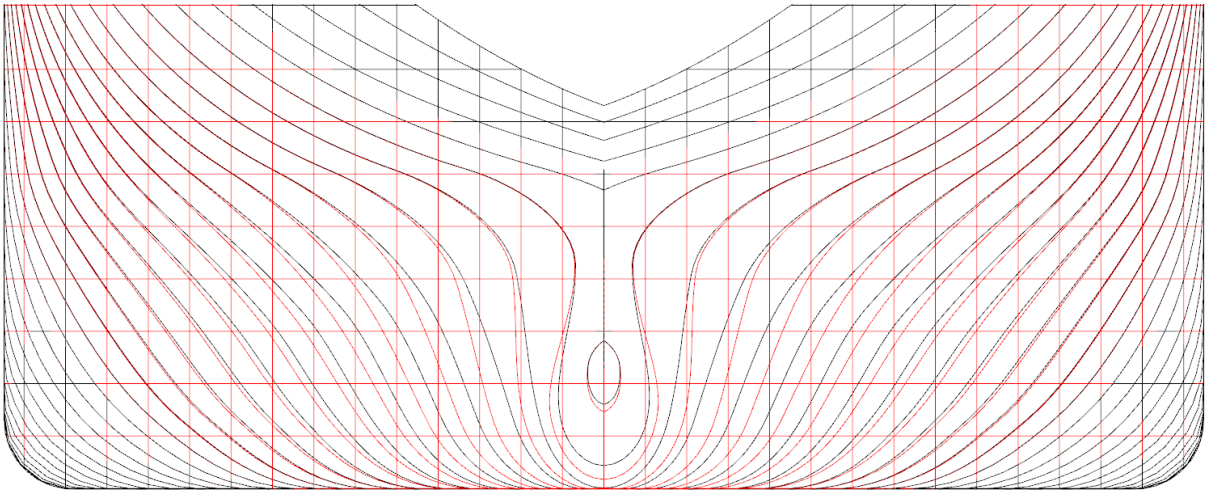

Figure 8: Geometry comparison of original (red) and modified (black) aftbody from CAD-based optimization

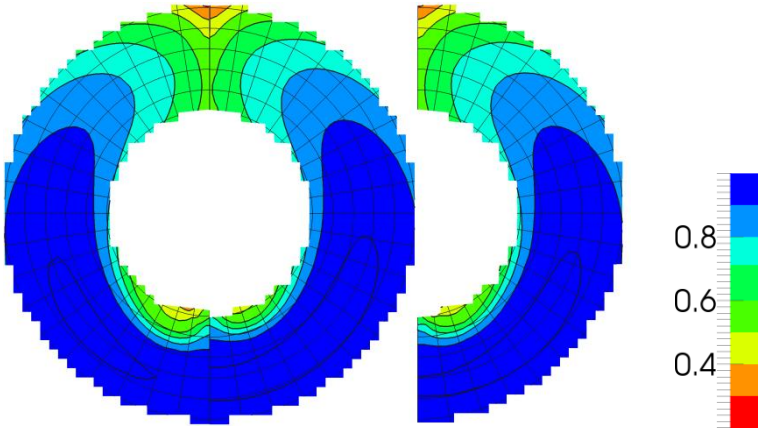

Figure 9: Wake fields: initial geometry left, final variant of CAD-based optimization middle, final variant of CAD-free optimization right

For validation purposes, the same aftbody optimisation task was performed with the previously mentioned CAD-free approach. Since the surface deformations due to this method strictly follow the adjoint shape sensitivity (apart from small local deviations due to smoothing/filtering), it provides valuable information for judging if the mapping of the shape sensitivities to the form parameters of the geometry carries enough information through to the modifications of the parametric model. Within the CAD-free optimisation procedure a smooth shape deformation is ensured by applying an explicit, consistent filtering approach. Here, a

filter width of 2.0m was used. In each optimisation step, the surface discretisation of the design object is adapted to the desired deformation; afterwards, the volume mesh is deformed by employing a PDE-based deformation method. For details on the employed method refer to [8].

The CAD-free optimisation study was started from the same primal reference case that was used for the CAD-based optimisation study. The maximum normal shape deformation per optimisation step was restricted to an absolute step size of 1cm, which was one magnitude smaller than in the CAD-based approach. The shape deformation was restricted to the aftship and constrained to account for the initial maximum draft and beam of the vessel. Furthermore, no change of the shape was allowed in the vicinity of the shaft line. In 35 optimisation steps the objective function value could be monotonically increased from 0.75103 to 0.75958 (see Figure 10).

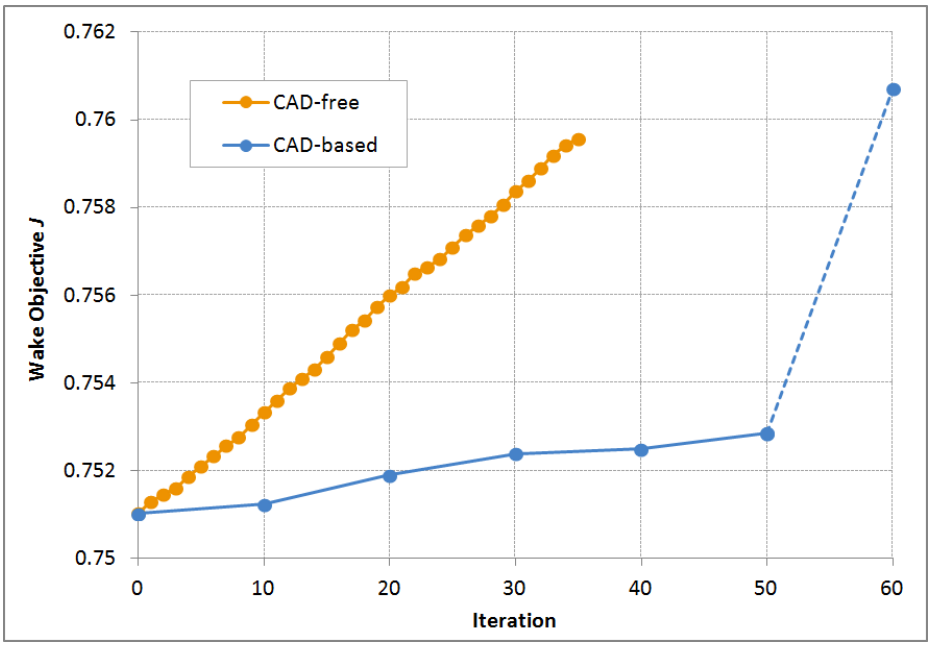

Figure 10: Geometry comparison of original (red) and modified (black) aftbody

Figure 10 shows a comparison of the optimization process between CAD-based and CAD-free approach. The objective values for the CAD-based approach are plotted in abscissa intervals of 10, to account for the 10-times bigger model surface displacement, when compared to the CAD-free approach. In this representation, one can see that within the same range of deformation (but, here, in more iterations) the CAD-free approach achieves a bigger improvement of the objective. This is most likely due to the fact that, by being detached from the shape's parameterization, it can follow the sensitivities much more exactly. Also, being applied to the full aftbody, the affected area was larger than for the CAD-based approach, which had been restricted to the skeg area only. It can be shown with these results, however, that the transfer of the adjoint shape sensitivities to the CAD model parameters has worked well and that the objective function can be improved in a continuous manner within an iterative process, making it easier to further process the optimized geometry in the

downstream design process.

5 CONCLUSIONS

Using adjoint CFD analysis methods and mapping the resulting shape sensitivities to the CAD model parameters allows an engineer to consider the biggest possible design space. All form parameters of the model can be involved into an optimization, without having to do a pre-selection. The expenses do not scale with the number of parameters. Actually, the sensitivities of all model parameters can even be determined quicker than for a subset using the direct approach.

One must consider, however, that the predictions based on the adjoint sensitivities are only valid for small (in strict mathematical sense infinitesimal) changes to the geometry. In practice, one would therefore have to proceed in an iterative way and compute new sensitivities for the respective modified geometry in multiple steps, improving the objective in small increments. This leads to the conclusion that the adjoint approach is especially applicable and efficient when dealing with high-dimensional design spaces.

AKNOWLEDGEMENT

Major parts of the work presented in this paper were realized within the research and development project No-Welle, funded by the Federal Ministry of Economics and Technology (BMWi) on the orders of the German Bundestag and PtJ as the conducting agency (FKZ 03SX362).

REFERENCES

[1] Harries, S. Investigating Multi-dimensional Design Spaces Using First Principle Methods. *7th International Conference on High-Performance Marine Vehicles (HIPER 2010)*, Melbourne, Florida, USA, 2010.

[2] Brenner, M., Abt, C. and Harries, S. Feature Modelling and Simulation-driven Design for Faster Processes and Greener Products. *International Conference on Computer Applications in Shipbuilding (ICCAS 2009)*, Shanghai, China, 2009.

[3] Kröger, J., Stück, A. and Rung, T. Adjoint Aftship Re-Design for Wake Optimisation under the Influence of Active Propulsion. *ECCOMAS Marine 2011*, Lisbon, Portugal, 2011.

[4] Rung, T., Wöckner, K., Manzke, M., Brunswig, J., Stück, A. and Ulrich, C. Challenges and Perspectives for Maritime CFD Applications. *Jahrbuch der Schiffbautechnischen Gesellschaft* (2009) **103**:127-139.

[5] Stück, A. *Adjoint Navier-Stokes Methods for Hydrodynamic Shape Optimisation*. PhD thesis, Hamburg University of Technology, 2012.

[6] Stück, A., Kröger, J. and Rung, T. Adjoint-based Hull Design for Wake Optimisation. *Ship Technology. Research* (2011) **58(1)**:34-44.

[7] Othmer, C. A continuous adjoint formulation for the computation of topological and surface sensitivities of ducted flows. *Int. J. Numer. Meth. Fluids* (2008) **58(8)**:861-877.

[8] Kröger, J. and Rung, T. CAD-free Hydrodynamic Optimisation Using Consistent Kernel-based Sensitivity Filtering. Submitted to *Ship Technology Research*, March 2, 2015.